Annals of Nuclear Medicine Vol. 15, No. 1, 79–83, 2001

Comparison of image reconstruction algorithms in myocardial perfusion scintigraphy

Jingming BAI,* Jun HASHIMOTO,* Takayuki SUZUKI,* Tadaki NAKAHARA,* Atsushi KUBO,* Shiro IWANAGA,** Hideo MITAMURA** and Satoshi OGAWA**

*Department of Radiology, School of Medicine, Keio University
**Department of Internal Medicine, School of Medicine, Keio University

The purpose of this study was to compare the clinical utility of two image reconstruction algorithms in myocardial perfusion SPECT (single-photon emission computed tomography): filtered back-projection (FBP) and ordered subset expectation maximization (OSEM). A rest/stress one-day protocol with ^{99m}Tc-MIBI or tetrofosmin was performed on 102 consecutive patients who underwent coronary angiography. After SPECT data acquisition, images were reconstructed with FBP and OSEM algorithms. We assessed diagnostic performance (sensitivity, specificity and accuracy) in detecting coronary artery stenosis and evaluated regional tracer uptake with a 4-point scoring system. Although there were no significant differences in diagnostic performance between FBP and OSEM reconstruction, the OSEM method yielded higher uptake in the RCA area than the FBP method by reducing the count-loss artifact due to hepatic uptake of the tracers. In addition, regional uptake in the LCX area was significantly lower in the OSEM image than in the FBP image; this phenomenon was observed mainly in patients with coronary stenosis and/or infarction in the LCX territory. In conclusion, OSEM and FBP offered comparable diagnostic performance in stress myocardial perfusion SPECT. The OSEM method contributed to reduction of the count-loss artifact in inferior and posterior walls and to easy recognition of hypoperfusion in the LCX area.

Key words: myocardial perfusion scintigraphy, image reconstruction, OSEM algorithm, Tc-99m-MIBI, Tc-99m-tetrofosmin

INTRODUCTION

MYOCARDIAL PERFUSION SPECT (single-photon emission computed tomography) is recognized as a crucial diagnostic method for coronary artery disease (CAD). Up to now, the conventional filtered back-projection (FBP) has widely been used in image reconstruction. Another reconstruction method, namely maximum likelihood expectation maximization (MLEM), is now being tested[1,2]; this method is able to incorporate various correction techniques, including scatter-, attenuation- and spatial resolution corrections. The disadvantage of the MLEM algorithm is that its formidable data processing requires longer calculation time. Nevertheless, recent advances in computer technology and the use of ordered subset expectation maximization (OSEM: a modified version of MLEM) reconstruction have provided acceptable calculation time in EM reconstruction.[3–8] To date, some authors have described the feasibility of the OSEM method in tumor and bone studies.[6,7] On the other hand, it seems that there is no report concerning clinical myocardial imaging. In this article, we compared diagnostic performance of the FBP and OSEM methods in stress myocardial perfusion scintigraphy with ^{99m}Tc labeled agents.

Received August 17, 2000, revision accepted January 6, 2001.

For reprint contact: Jun Hashimoto, M.D., Department of Radiology, School of Medicine, Keio University, 35 Shinanomachi, Shinjuku-ku, Tokyo 160–8582, JAPAN.
E-mail: junhashi@rad.med.keio.ac.jp

MATERIALS AND METHODS

Patients

We analyzed the data of 102 consecutive patients (male 85, female 17, 61.8 ± 13.8 years of age) who underwent

Table 1 Diagnostic performance of FBP and OSEM reconstructions

	Sensitivity			Specificity			Accuracy		
	FBP	OSEM	p value	FBP	OSEM	p value	FBP	OSEM	p value
LAD	57%	55%	ns	95%	98%	ns	72%	72%	ns
RCA	73%	71%	ns	88%	90%	ns	80%	80%	ns
LCX	64%	69%	ns	92%	88%	ns	80%	80%	ns
Total	64%	64%	ns	91%	91%	ns	77%	77%	ns

(p value: FBP vs. OSEM; n = 102 patients, 306 coronary arteries)

coronary angiography (CAG). Of the 102 patients, 78 were referred for ergometer exercise and 24 dipyridamole test. Angiographic findings indicated that 20 patients had no significant stenosis, 31 had one-vessel disease, 28 had two-vessel disease and 23 had three-vessel disease. The patients consisted of 38 with myocardial infarction and 64 without infarction.

Written informed consent was obtained from all patients after they received a detailed explanation of the examination. The form of the explanation was approved by the institutional committee of Keio University Hospital.

Protocol

We employed a rest/stress one-day protocol with ^{99m}Tc-MIBI or tetrofosmin. Patients were fasted before the first injection. Rest imaging started 30 minutes after the first injection of 300 MBq of the tracers and stress imaging started 30 minutes after the second injection of 900 MBq.

Data acquisition and image processing

All images in this investigation were acquired with a three-headed rotating gamma camera equipped with parallel-hole collimators (GCA-9300A/HG, Toshiba Corporation, Tokyo) and processed with a medical image processor (GMS-5500A/DI, Toshiba Corporation, Tokyo). SPECT data were acquired for 15 minutes by 120-degree continuous rotation of each detector (360-degree acquisition). The raw data were converted to 90 projections stepped by 4 degrees, which were reconstructed into 128 × 128 matrix images.

In FBP reconstruction, after processing with a Butterworth filter (order: 8, cut-off frequency: 0.15 cycles/pixel), data were reconstructed with a ramp filter. In OSEM reconstruction, a Butterworth filter (order: 8, cut-off frequency: 0.17 cycles/pixel) was used as a preprocessing filter. As for the iteration times and subset configuration for the OSEM reconstruction algorithm, it seems no general agreement has yet been reached. According to most studies concerning phantom experiments and clinical applications to other organs, iterations ranging from 3 to 5 supplied with more than 8 views per subset were used.[8-11] In this study, OSEM reconstruction was carried out with 3 iterations and 9 subsets which contains 10 views per subset. Since appropriate methods for attenuation correction incorporated in OSEM reconstruction were not available, we did not perform attenuation correction in the present study.

Table 2 Comparison of perfusion scores between FBP and OSEM images

		FBP	OSEM	p value
LAD	stress	2.25 ± 1.02	2.28 ± 1.04	ns
	rest	2.27 ± 0.93	2.32 ± 0.95	ns
RCA	stress	1.48 ± 0.79	1.59 ± 0.84	0.0271
	rest	1.44 ± 0.77	1.54 ± 0.78	0.0494
LCX	stress	2.48 ± 0.81	2.39 ± 0.85	0.0283
	rest	2.60 ± 0.74	2.48 ± 0.78	0.0067

(p value: FBP vs. OSEM)

Table 3 Patient-based differences between FBP and OSEM methods

		OSEM > FBP	FBP = OSEM	OSEM < FBP
LAD	stress	5	95	2
	rest	8	91	3
RCA	stress	15	82	5
	rest	16	81	5
LCX	stress	2	88	12
	rest	4	85	13

(OSEM > FBP: OSEM images show higher uptake than FBP images; FBP = OSEM: Uptakes in FBP and OSEM images are same; OSEM < FBP: OSEM images show lower uptake than FBP images)

Image interpretation

Stress and rest short axial images were read independently by two experienced doctors. The doctors were not informed of CAG findings of the patients. When the two doctors made different diagnoses, the final diagnosis was decided by discussion. For semi-quantitative analysis, the myocardium was divided into 3 vascular territories: LAD, RCA and LCX areas. We assigned a perfusion score to each area. The perfusion score was determined by using a 4-point scoring system (3 to 0 for normal to defect). If one vascular territory contained two or more portions with different scores, the lowest score was assigned to the territory. In other words, the score in zones manifesting the most reduced uptake in the coronary territory was used for evaluation.

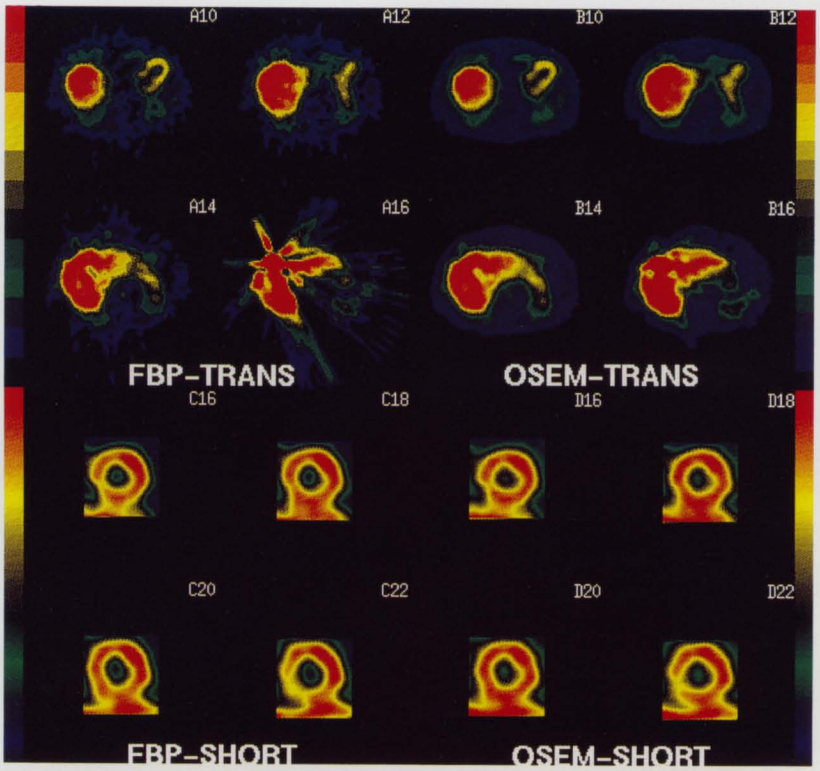

Fig. 1 SPECT images of a patient without coronary stenosis. Upper left, FBP transverse images; upper right, OSEM transverse images; lower left, FBP short-axis images; lower right, OSEM short-axis images.

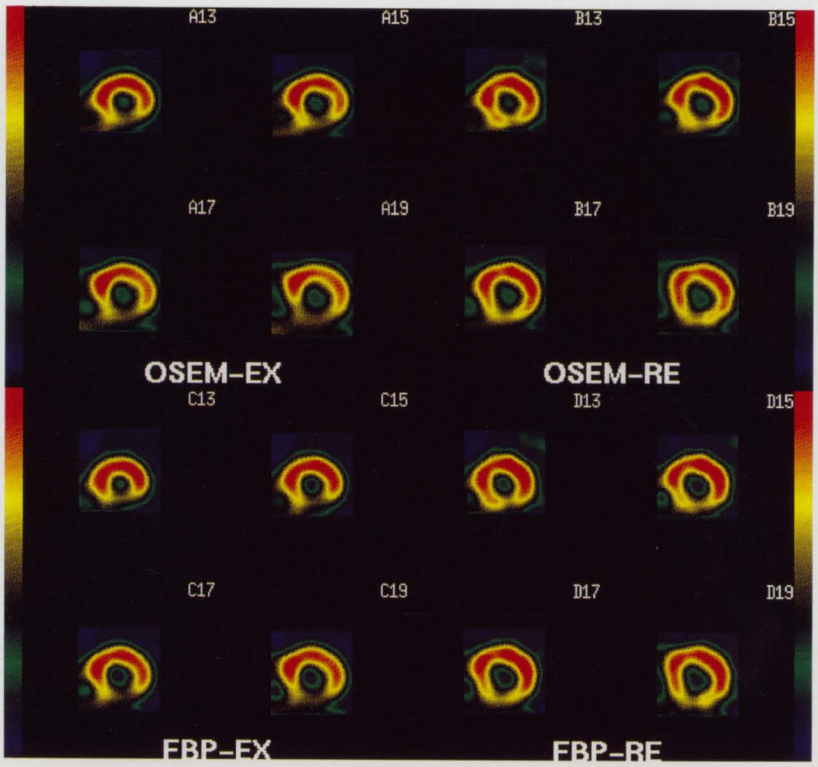

Fig. 2 Short axial images of a patient with lateral and inferoposterior ischemia. Upper left, OSEM stress images; upper right, OSEM rest images; lower left, FBP stress images; lower right, FBP rest images.

Data analysis

We assessed sensitivity, specificity and accuracy for detecting coronary artery stenosis on the basis of visual interpretation of images reconstructed by FBP and OSEM. The results of CAG were used as the gold standard in diagnosing CAD; stenosis exceeding 50% of the lumen diameter (AHA 75%) was considered significant. Mean perfusion scores were also calculated in images reconstructed by the two methods.

Statistics

The chi-square test or Fisher's exact test was used to compare the sensitivity, specificity and accuracy of FBP and OSEM reconstructions. We used the paired t-test to compare perfusion scores of FBP and OSEM images. A p-value < 0.05 was considered significant.

RESULTS

Sensitivity, specificity and accuracy of FBP and OSEM reconstruction algorithms are summarized in Table 1. There were no significant differences between FBP and OSEM reconstruction in diagnostic performance. Relatively low sensitivity and high specificity were observed regardless of the reconstruction method.

Measured perfusion scores are indicated in Table 2. The OSEM algorithm yielded significantly higher scores in the RCA area and lower scores in the LCX area than with the FBP algorithm. Table 3 reveals patient-based differences between the two reconstruction methods.

Figure 1 shows rest SPECT images obtained from a 69-year-old male with angina pectoris. Coronary angiography revealed no significant stenosis. Compared with FBP images, OSEM reconstruction reduces the streak artifact (upper panels) and the count-loss artifact (lower panels) due to hepatobiliary accumulation. Measured inferior-to-anterior count ratios were 0.87 and 0.97 in FBP and OSEM images, respectively.

Figure 2 shows images of a 74-year-old male with angina pectoris. Coronary angiography revealed 90% stenosis in both LCX and RCA. Although decreased perfusion is observed in both FBP and OSEM stress images, the abnormality in the LCX area is recognized more easily in OSEM images than in FBP images. Measured lateral-to-anterior count ratios were 0.94 and 0.89 in FBP and OSEM images, respectively.

DISCUSSION

Myocardial perfusion tomography with MIBI and tetrofosmin, as well as ^{201}Tl, is playing an important role in diagnosing coronary artery disease. To date, SPECT reconstruction by filtered back-projection is still performed widely. This process, first described by Shepp and Logan, convolves projection data with filter function which creates a band of negative pixels immediately around hot objects to eliminate artifacts,[12] but many investigators reported limitations of FBP reconstruction, especially the count-loss artifact caused by liver uptake of the tracers.[13–16] The OSEM algorithm is expected to be useful in eliminating the count-loss artifact. In this article, we compared FBP and OSEM algorithms qualitatively and semi-quantitatively in clinical myocardial SPECT with ^{99m}Tc labeled perfusion agents.

We qualitatively evaluated sensitivity, specificity and accuracy in diagnosing coronary artery stenosis. None of the results based on coronary artery areas showed any significant difference between the two reconstruction methods (Table 1).

Although the qualitative analysis did not show any significant difference, in semi-quantitative analysis, uptake in the RCA area obtained from FBP images was significantly lower than that from OSEM, whereas uptake in the LCX area obtained from FBP was significantly higher than that from OSEM. The cause of the difference between FBP and OSEM algorithms in the RCA uptake is thought to lie in the FBP itself which draws out negative pixels around the hot area (Fig. 1). Filtering projection with a ramp generates the above negative pixel values near the liver, resulting in reduced counts in the inferior and posterior myocardial walls.[13–16] In contrast, the OSEM algorithm automatically suppresses the artifact by its inherent non-negativity constraint; this feature was demonstrated by a phantom experiment with the MLEM algorithm.[16] Table 3 shows that 15 patients at stress and 16 patients at rest had higher uptake in the RCA area in OSEM images than in FBP images. Of the above 16 patients, coronary angiography revealed intact RCA in 9 patients. FBP images showed perfusion scores of 2 or 1 in all of the 9 patients, meanwhile OSEM images showed a score of 3 in 7 of the 9 patients ($p = 0.0023$, Fisher's exact method). This result also suggests that the OSEM procedure compensates for the count-loss in the inferior and posterior walls, but the effect of OSEM had no influence on overall diagnostic accuracy (Table 1); this is due to our image interpretation considering the effects of photon attenuation and the count-loss in the inferior and posterior walls. For example, when a patient manifested normal inferoposterior uptake in the stress image and reduced uptake in the rest image because of the count-loss, we diagnosed this condition as normal.

In the LCX area, the perfusion scores in images processed with OSEM were significantly lower than those processed with FBP (Table 2, Fig. 2). Comparing FBP and OSEM images, discrepancies in the LCX area were found in 14 patients at stress and 17 patients at rest (Table 3). Twelve of the 14 patients at stress and 13 of the 17 patients at rest showed relatively lower uptake when processed with the OSEM algorithm. Among all these discrepant cases, most (8/12 at stress and 9/13 at rest) were found to suffer from coronary stenosis and/or myocardial infarction in the LCX territory. The findings might be important

in the diagnosis of CAD, because the relatively low uptake allows easy diagnosis of hypoperfusion in the LCX area. A possible reason for the phenomenon in OSEM reconstruction is relatively increased tracer uptake in the RCA area (detailed in the previous paragraph) which enhances the findings of decreased uptake in the LCX area, but the increased inferoposterior uptake in the OSEM image cannot completely explain the reduced lateral uptake in the case presented in Figure 2. Further studies are required to clarify other factors related to the low score in the LCX area.

Another noticeable point in the present study is that uptake at stress was higher than that at rest in the RCA area. To clarify the reasons for this phenomenon in the RCA area, we investigated hepatic uptake of the tracers in stress and rest images. Higher stress uptake than rest uptake in the RCA area was observed in 16 (FBP) and 11 (OSEM) patients. Of the above patients, 81% manifested hepatic accumulation equal to or higher than myocardial uptake in the rest image, whereas only 30% showed it in the stress image. Accordingly, the count-loss artifact caused by the relatively high liver accumulation at rest is thought to be one of the reasons for the lower uptake in the RCA area at rest.

Although the OSEM method reduces calculation time significantly, it takes a longer time to reconstruct images than the conventional FBP method. In our study, the FBP and OSEM methods required about 20 seconds and 2 minutes to generate transaxial images, respectively. Furthermore, incorporation of various correction procedures, one of the advantages of the OSEM method, is not often implemented because of the lack of clinically available programs. These shortcomings of the OSEM method have prevented widespread acceptance of the method.

In summary, we compared the clinical utility of FBP and OSEM reconstruction algorithms on the basis of diagnostic performance and the perfusion score. Although there was no significant difference in sensitivity, specificity or accuracy in each coronary artery area, perfusion scoring analysis revealed significantly higher uptake in the RCA region and lower uptake in the LCX region in the OSEM image than in the FBP image. The higher uptake in the RCA area is related to the reduction of the count-loss due to increased hepatic accumulation, and relatively low uptake in the LCX area assists the recognition of hypoperfusion.

ACKNOWLEDGMENT

Jingming Bai is supported by Japan International Cooperation Agency (JICA).

REFERENCES

1. Lange K, Carson R. EM reconstruction algorithms for emission and transmission tomography. *J Comput Assist Tomogr* 1984; 8: 306–316.
2. Floyad CE Jr, Jaszczak RJ, Coleman RE. Convergence of the maximum likelihood reconstruction algorithm for emission computed tomography. *Phys Med Biol* 1987; 32: 463–476.
3. Reader AJ, Visvikis D, Erlandsson K, Ott RJ, Flower MA. Intercomparison of four reconstruction techniques for positron volume imaging with rotating planar detectors. *Phys Med Biol* 1998; 43: 823–834.
4. Hutton BF, Accarne BV. Efficient scatter modeling for incorporation in maximum likelihood reconstruction. *Eur J Nucl Med* 1998; 25: 1658–1665.
5. Hutton BF, Lau YH. Application of distance-dependent resolution compensation and post-reconstruction filtering for myocardial SPECT. *Phys Med Biol* 1998; 43: 1679–1693.
6. Lonneux M, Borbath I, Bol A, Coppens A, Sibomana M, Bausart R, et al. Attenuation correction in whole-body FDG oncological studies: the role of statistical reconstruction. *Eur J Nucl Med* 1999; 26: 591–598.
7. Blocklet D, Seret A, Popa N, Schoutens A. Maximum-likelihood reconstruction with ordered subsets in bone SPECT. *J Nucl Med* 1999; 40: 1978–1984.
8. Dey D, Slomka PJ, Hahn LJ, Kloiber R. Comparison of ordered subsets expectation maximization and Chang's attenuation correction method in quantitative cardiac SPECT: a phantom study. *Nucl Med Commun* 1998; 19: 1149–1157.
9. Lonneux M, Borbath I, Bol A, Coppens A, Sibomana M, Bausart R, et al. Attenuation correction in whole-body FDG oncological studies: the role of statistical reconstruction. *Eur J Nucl Med* 1999; 26: 591–598.
10. Case JA, Licho R, King MA, Weaver JP. Bone SPECT of the spine: a comparison of attenuation correction techniques. *J Nucl Med* 1999; 40: 604–613.
11. Lalush DS, Tsui BMW. Performance of ordered-subset reconstruction algorithms under conditions of extreme attenuation and truncation in myocardial SPECT. *J Nucl Med* 2000; 41: 737–744.
12. Shepp L, Logan B. The Fourier reconstruction of a head section. *IEEE Trans Nucl Sci* 1974; 21: 21–43.
13. Germano G, Chua T, Kiat H, Areeda JS, Berman DS. A quantitative phantom analysis of artifacts due to hepatic activity in technetium-99m myocardial perfusion SPECT. *J Nucl Med* 1994; 35: 356–359.
14. King MA, Xia W, delVries DJ, Pan TS, Villegas BJ, Dahlberg S, et al. A Monte Carlo investigation of artifacts caused by liver uptake in single-photon emission computed tomography perfusion imaging with technetium 99m-labeled agents. *J Nucl Cardiol* 1996; 3: 18–29.
15. Matsunari I, Tanishima Y, Taki J, Ono K, Nishide H, Fujino S, et al. Early and delayed technetium-99m-tetrofosmin myocardial SPECT compared in normal volunteers. *J Nucl Med* 1996; 37: 1622–1626.
16. Nuyts J, Dupont P, Maegdenbergh VV, Vleugels S, Suetens P, Mortelmans L. A study of the liver-heart artifact in emission tomography. *J Nucl Med* 1995; 36: 133–139.